Journal of Solid State Chemistry 182 (2009) 1351–1358

Contents lists available at ScienceDirect

Journal of Solid State Chemistry

journal homepage: www.elsevier.com/locate/jssc

Effect of silver on phase separation and crystallization of niobium oxide containing glasses

H. Smogor [a], T. Cardinal [a,*], V. Jubera [a], E. Fargin [a], J.J. Videau [a], S. Gomez [b], R. Grodsky [a], T. Denton [a], M. Couzi [c], M. Dussauze [c]

[a] CNRS, Université de Bordeaux, ICMCB, 87 av. Dr. A. Schweitzer, Pessac F-33608, France
[b] Université de Bordeaux, CREMEM, Talence F-33405, France
[c] ISM, UMR 5803 CNRS, Université Bordeaux, 351 cours de la libération, Talence F-33405, France

ARTICLE INFO

Article history:
Received 1 December 2008
Received in revised form
20 February 2009
Accepted 27 February 2009
Available online 6 March 2009

Keywords:
Glass
Crystallization
Nucleation agent
Niobium oxide

ABSTRACT

Effect of silver introduction in sodium phosphate and sodium borophosphate glasses containing large amount of niobium oxide have been investigated using differential scanning calorimetry and XRD. Same sodium niobate phase in the Nb_2O_5–$NaNbO_3$ based solid solution have been observed following two heat treatments designed for nucleation and growth of the crystalline phase. Silver introduction in the glass composition is clearly responsible for increasing the crystallization rate. Its effect after nucleation and crystallization treatments has been shown. Phase metastable separation is occurring during heat treatment with formation of a phosphate rich and niobium rich phase. Crystallization effect on optical transparency of glasses and on Raman scattering response have been investigated.

1. Introduction

Transparent materials exhibiting NLO properties are attracting attention for the development of integrated optics. For such purpose, glass ceramics could become key materials if homogeneous devitrification control can be achieved to preserve optical transparency. The two main criteria are to maintain small crystal size as compared to the optical wavelength or to have adaptation of linear refractive indices between the glass host and the crystalline phase [1]. Glasses containing large amount of d^0 ions have been investigated for application in optics for 20 years [2]. Precipitation of titanate and niobate crystalline phases has been studied in different glass systems mainly in silicates and germanates [3–5]. In the case of niobium oxide, large amount of this oxide can be introduced in different glass systems and especially in phosphate and borophosphate matrices leading to significant NLO optical properties such as Kerr effect or SHG after thermal poling [6]. For niobium oxide loading, the presence of a 3D network of NbO_6 octahedra which could be compared to tungsten bronze crystalline structure, has been shown to give important contribution to the optical Kerr coefficient [7]. In such glasses, sodium niobate phases have been reported to precipitate after thermal treatment above the glass transition temperature [8]. Since glass ceramic materials are suspected to offer even larger NLO response, transparency in the optical region of interest is desirable. For such a goal, the control of the size and the homogeneous dispersion of the crystallites are key issues.

First of all, crystallization has to be internal as opposed to surface one's. Secondly numerous crystallites centres are desired. Different approaches have been developed in order to obtain such glass ceramic. One of the main ways is to introduce nucleating agent. Many studies have been devoted to such subject. Cations or/and anions have been introduced in different glass matrices in order to control and to monitor glass ceramic formation such as transition ions (Cr^{3+}), rare earth ions, fluorine [9,10]. Silver ion is well known for its ability to form clusters or metallic particles after heat treatment or radiation exposure. Combination of light and heat treatment as Stookey demonstrated was at the base of photochromic glasses or hologram recording [11,12].

In the present work, the influence of silver introduction on the crystallization of sodium niobate phase has been investigated in sodium phosphate and borophosphate glass matrices. Phosphate and borophosphate matrices, studied in this paper, have been previously reported for insuring the introduction of large amount of d^0 ions [13]. Behaviours of such glasses toward crystallization are compared. Nucleation and crystallization processes have been conducted and the crystallization phases have been identified. Resulting transmission optical spectra and Raman response of the composite material are reported.

2. Experimental

Niobium oxide containing glasses have been elaborated using standard melting routes. Two different glass matrices $NaPO_3$ and

* Corresponding author. Fax: +33 5 4000 2761.
E-mail address: cardinal@icmcb-bordeaux.cnrs.fr (T. Cardinal).

0022-4596/$ - see front matter © 2009 Elsevier Inc. All rights reserved.
doi:10.1016/j.jssc.2009.02.028

$0.95NaPO_3$+0.05 $Na_2B_4O_7$ with 0.42 molar fraction of Nb_2O_5 were prepared using $NaPO_3$ (Aldrich) $Na_2B_4O_7$ (Aldrich) and Nb_2O_5 (Alfa Aesar) raw materials. The powders after heat treatment, respectively, at 300, 530 and 800 °C for moisture removing were mixed and placed in a platinum crucible with appropriate amount. For each composition, two different glasses have been prepared, a virgin sample and a glass with 0.005 molar fraction of Ag_2O in order to compare the influence of silver on crystallization behaviour. $AgNO_3$ (Alfa Aesar) powder was used as raw material and mixed with the appropriate amount of the other raw materials prior melting. Melting in platinum crucible was performed around 1200 °C followed by fast quenching on brass mold. Annealing of the resulting glass sample was performed at 30 °C below the glass transition temperature for 15 h.

Glass transition temperatures were measured using DSC calorimeter Netzsch 404. Signals collected with empty platinum crucibles were systematically subtracted to the data. Heating rates of 10 °C/min have been chosen for all measurements. Signals have been recorded for about 10 mg of glass powder. Glass transition temperatures were defined by the onset on the first change of slope corresponding to the glass transition phenomenon. The temperatures T_x have been defined as the onset of the change of slope of the crystallization exothermic phenomenon. The T_c is defined as the maximum of the peak corresponding to crystallization peak. The error on temperature measurement due to calibration is estimated to ± 1 °C and the error due to determination of onset and maxima is estimated to ± 2 °C. The total error is ± 3 °C.

For, respectively, nucleation and crystallization heat treatments, temperatures have been defined, respectively, near the inflection point corresponding to the glass transition phenomena and about 60 °C below the T_x temperature.

X-ray diffraction (XRD) data have been collected on a PANalytical X'Pert Pro instrument using the Cu$K\alpha$1 radiation.

Absorption spectra were recorded using a double beam spectrophotometer (CARY 5000 UV–VIS–NIR) between 200 and 800 nm.

Raman spectra were recorded at room temperature on a LabRam confocal micro-Raman instrument (Jobin–Yvon), using backscattering geometry and a typical resolution of 2–3 cm^{-1}. The system consists of a holographic notch filter for Rayleigh rejection, a microscope equipped with 10×, 50× and 100× objectives (the latter allowing a spatial resolution of less than 2 μm), and a CCD detector. The 514 nm emission line of an argon–krypton laser was used for excitation.

Electron microscopy micrograph has been collected using HRSEM JEOL 6700F (gun field emission—resolution 1.1 nm). Acceleration voltage was at 5 kV. Gold flash deposition technique has been used to avoid surface charging effects.

3. Results

In Table 1 are reported the different treatment and codes used along the paper.

3.1. Thermal analysis

The DSC data collected are presented in Fig. 1 for phosphate ($NaPO_3$) and borophosphate ($0.95NaPO_3$+$0.05Na_2B_4O_7$) matrices, respectively, reported as PN42 and BPN42. Labelling for silver containing glasses is the following: PN42Ag and BPN42Ag. The DSC curves for both PN42 and BPN42 compositions exhibit similar shapes with an endothermic signal corresponding to the glass transition and exothermic features with two peaks corresponding to crystallization phenomena. It has been recently demonstrated that the first phase at lower temperature is a sodium niobate phase while the second phase corresponds to $Na_4Nb_8P_4O_{32}$ [8].

In Table 2 are reported the glass transition temperature and the T_x temperature corresponding to the onset of the crystallization phenomenon as well as the maximum of the two crystallization peaks. The errors on the measurements come from temperature calibration using melting of reference samples as well as error on determination of the onsets and the maxima. In Table 2 are reported the errors due to determination of the onsets and the maxima. As compared to borophosphates, glass transition phenomenon and crystallization features of the phosphate glasses appear at higher temperature and the difference T_x-T_g is lower. DSC curves on undoped and silver doped glasses are reported in Fig. 1b and c. In the insert are shown the derivative of the DSC curves.

DSC signal have been collected after the nucleation thermal treatment above the T_g (3 h heat treatment at 640 or at 690 °C, respectively, for borophosphate and phosphate matrices). One has to mention that after the nucleation treatment no crystallization could be noticed using XRD. Similar DSC features have been recorded for all doped glasses as compared to the virgin glass without silver and without heat treatment. In both cases for phosphate and borophosphate glasses, no significant effect of silver addition on glass transition temperatures can be noticed according to the DSC measurement error bars. Changes are clearly visible on crystallization peak positions. Silver presence induces a decrease of crystallization onset T_x for both glass systems as well as a decrease of the temperature corresponding to the maximum of the crystallization peaks T_{c1} and T_{c2}. As seen on the inserts, the derivative of the DSC signal indicates that inflection point positions follow the same trend. As a result, the difference T_x-T_g decreases for silver containing glasses indicating that such ions facilitate the crystallization. After nucleation heat treatments, smaller T_x-T_g differences are achieved. On data not shown here, the effect of the nucleation heat treatment is less effective for silver free samples in terms of reducing the T_x-T_g difference.

3.2. X-ray diffraction

XRD patterns have been collected, after nucleation heat treatment followed by different second thermal treatment, in order to identify the nature of the crystalline phases and to evaluate the kinetic of its formation. The second heat treatment corresponding to crystallization has been defined at 720 and

Table 1
Different treatments and codes used along the paper for the different samples.

Glass composition	Comments	Code
0.551 $NaPO_3$+0.029 $Na_2B_4O_7$+0.42 Nb_2O_5	Annealed	BPN42
0.995 (0.551 $NaPO_3$+0.029 $Na_2B_4O_7$+0.42 Nb_2O_5)+0.5 Ag_2O	Annealed	BPN42Ag
0.995 (0.551 $NaPO_3$+0.029 $Na_2B_4O_7$+0.42 Nb_2O_5)+0.5 Ag_2O	Annealed and heat nucleated 3 h at 640 °C	BPN42Ag(3 h)
0.58 $NaPO_3$+0.42 Nb_2O_5	Annealed	PN42
0.995 (0.58 $NaPO_3$+0.42 Nb_2O_5)+0.5 Ag_2O	Annealed	PN42Ag
0.995 (0.58 $NaPO_3$+0.42 Nb_2O_5)+0.5 Ag_2O	Annealed and heat nucleated 3 h at 670 °C	PN42Ag(3 h)

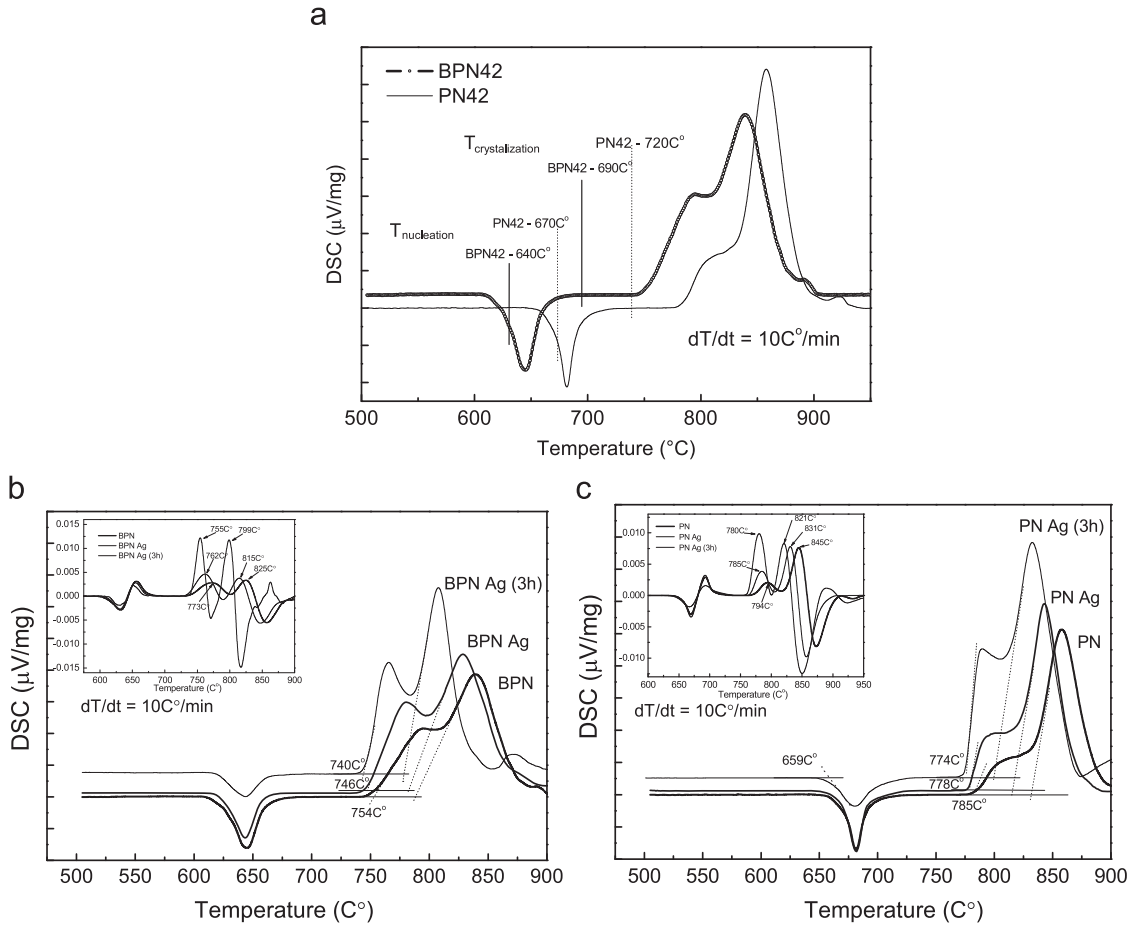

Fig. 1. DSC signal collected on sodium and niobium phosphate or borophosphate glasses (a), for borophosphates (b) and phosphates (c) undoped and doped with silver ions and following 3 h nucleation heat treatment.

Table 2
Glass transition temperature (T_g), onset of the first crystallization peak (T_x), and difference between T_g and T_x (T_x–T_g) and maximum of the crystallization peaks (T_c).

Glass	T_g (°C) (±2 °C)	T_x (°C) (±2 °C)	T_x–T_g (°C) (±4 °C)	T_{c1} (°C) (±2 °C)	T_{c2} (°C) (±2 °C)
NP42	665	785	120	811	858
NP42Ag	663	778	115	801	842
NP42Ag (3 h)	662	774	112	789	832
BPN42	624	754	130	795	840
BPN42Ag	624	746	122	780	828
BPN42Ag (3 h)	622	740	118	765	807

690 °C, respectively, for phosphate and borophosphate matrices, about 60 °C below T_x of silver undoped glasses. These treatments have been conducted for different durations for each sample. XRD patterns have been collected for each material after grinding the samples into fine powder and sifting at 30 μm to obtain a homogeneous size powder. A long time acquisition (30 s per step of 0.02° in 2θ) was used to optimize the signal over noise ratio of the diffractograms. In order to identify the crystalline phases formed, the well-known materials $NaNbO_3$ [14] (orthorhombic unit cell with $a = 5.5679$, $b = 15.5156$ and $c = 5.5029$, space group *Pbma*), $Na_4Nb_8P_4O_{32}$ (monoclinic unit cell with $a = 6.635$, $b = 5.352$, $c = 17.967$ and $\beta = 90.33$, space group $P2_1$) [15] and $Na_{13}Nb_{35}O_{94}$ (orthorhombic unit cell with $a = 12.363325$, $b = 37.029984$, $c = 3.953664$, space group *Pba*2) [16], have been prepared using solid state reaction. The structure of $Na_{13}Nb_{35}O_{94}$ (*t*-TTB) compound corresponds to a tripled unit cell of the basic tetragonal tungsten bronze $NaNb_3O_8$ (TTB) along the [010] direction. The geometry of the ferroelectric domains of this phase was described by Craig et al. The purity of these compounds was checked using a pattern matching routine refinement [17]. Their diffractograms were used as references and compared with glass ceramic XRD patterns after a 3 h nucleation treatment and different heat treatments of 9.5 and 75 h. The analysis is in concordance with results obtained by Malakho et al. In the borophosphate matrix containing between 43 and 48 mol% of Nb_2O_5, they have attributed the first crystallization to the formation of TTB in the system Nb_2O_5–$NaNbO_3$, while the second phase is $Na_4Nb_8P_4O_{32}$ [8].

The short crystallization heat treatments of the PN42 and BPN42 compositions favour the precipitation of the same crystalline phase (Fig. 2a and b). In order to evaluate the kinetic of its formation, several durations of these second heat treatments have been conducted. In the borophosphate matrix case, crystallization peaks appear for a 2.5 h thermal treatment while for phosphate matrix similar features can be observed at 4.5 h. Above those durations, they are clearly visible in Fig. 2a and b. For both glass systems, diffraction patterns are identical at the first stage of the crystallization and correspond to the phase $Na_{13}Nb_{35}O_{94}$ (see reference diffraction patterns in Fig. 3a and b). The introduction of silver makes possible a crystallization at an earlier

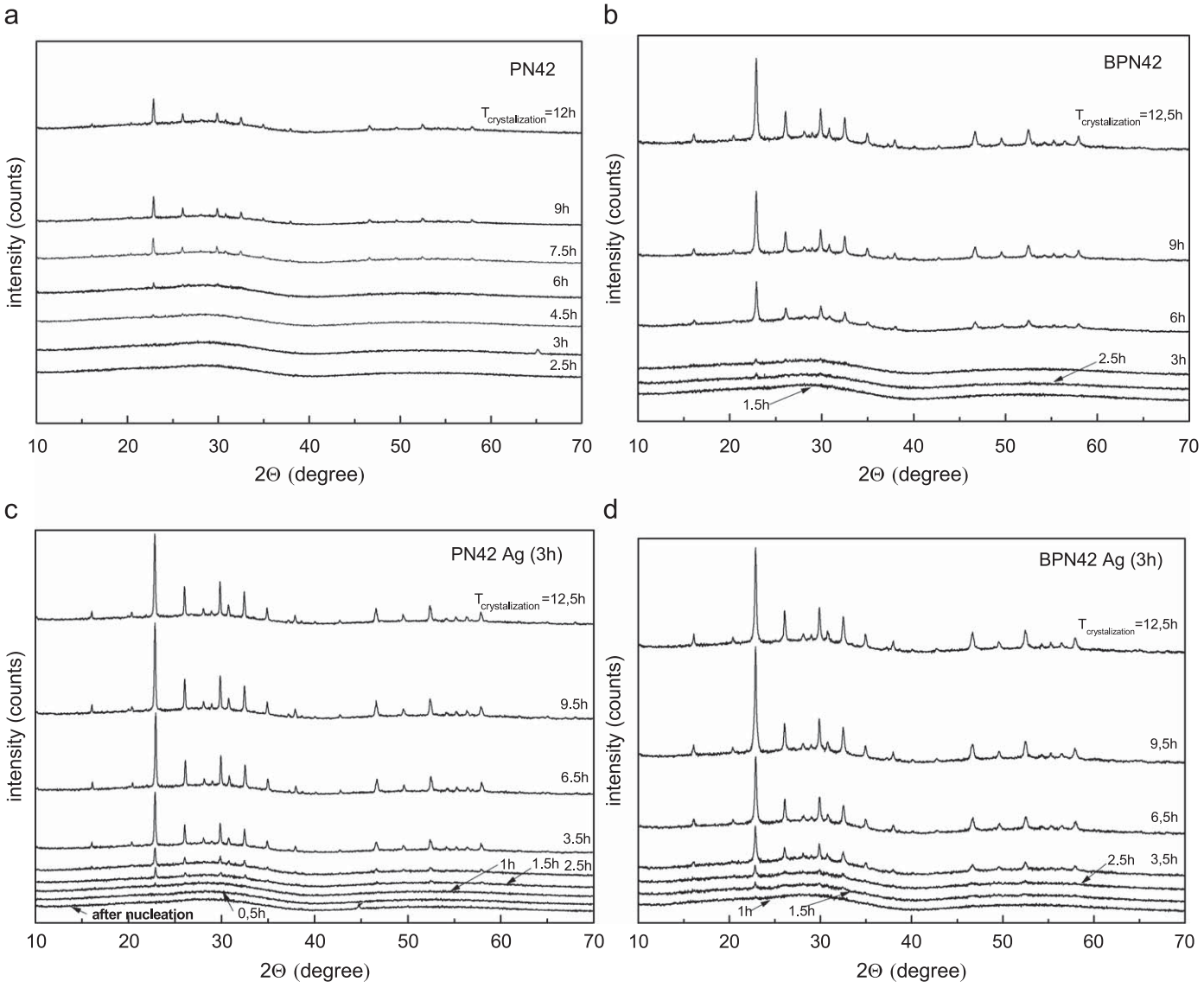

Fig. 2. XRD patterns for same nucleation heat treatment respectively for sodium–niobium phosphates (a) and borophosphates (b), and for silver doped phosphates (c) and borophosphates (d) after 3 h nucleation heat treatment for different crystallization heat treatment durations.

stage for both PN42Ag and BPN42Ag glasses and does not modify the nature of crystalline phases precipitated in the glassy host (data for glass with first 3 h heat treatment are presented in Fig. 2c and d).

For very long second thermal treatment duration (75 h), new diffraction peaks appear, revealing the presence of $Na_4Nb_8P_4O_{32}$ in high proportion (Fig. 3c and d). Because of the versatility of crystalline compounds in the B–P–Nb–Na–O phase diagrams, other non-identified secondary phases are also detected in small proportion, in the XRD pattern. The precipitation of $Na_4Nb_8P_4O_{32}$ occurs first in the borophosphate matrix. The diffraction pattern observed corresponds to the results obtained by Malakho et al. for high niobium oxide in borophosphate matrix. After a 75 h heat treatment, $Na_{13}Nb_{35}O_{94}$ (*t*-TTB) is still detected in the phosphate glassy matrix but not in the borophosphate host.

To better understanding the nucleation-growth process of *t*-TTB, evolution of the diffraction peak located at $2\theta = 22.9^\circ$ which corresponds the highest peak intensity has been studied. As no overlap exists with the XRD pattern of $Na_4Nb_8P_4O_{32}$, we have investigated the integrated area under the diffraction line versus different heat treatment durations. The corresponding results are reported in Fig. 4a and b. For BPN42Ag (3 h) and PN42Ag (3 h) crystalline signature can be seen on the diffraction pattern immediately after 1 h of second heat treatment. One can also observe that, as expected from the XRD patterns shown in Fig. 2, the $Na_{13}Nb_{35}O_{94}$ crystalline phase grows first in these two glasses while the other materials (Ag-free glasses and no heat nucleated glasses) exhibit slower slopes. This effect can be correlated with the slope of the DSC curve described in Fig. 1a and b. For both phosphate and borophosphate hosts, the shape of the curves in Fig. 4a and b are similar. A fit using polynomial function is also reported for eye guiding. The evolution of 22.9° peak area of PN42Ag (3 h) and BPN42Ag (3 h) first present a sharp increase after few hours of second heat treatment followed by a slow down. This effect can be seen in Fig. 4c by looking at the derivative curve which gives a maximum at 2.8 and 3.2 h for PN42Ag (3 h) and BPN42Ag (3 h), respectively. For compositions without heat nucleation, crystallization starts later. The role of silver on crystallization is confirmed by a higher rate of formation of the sodium niobate phase. For the longest second heat treatment duration, the decrease of the 22.9° peak area is correlated with the precipitation and growth of $Na_4Nb_8P_4O_{32}$. After 75 h, as described

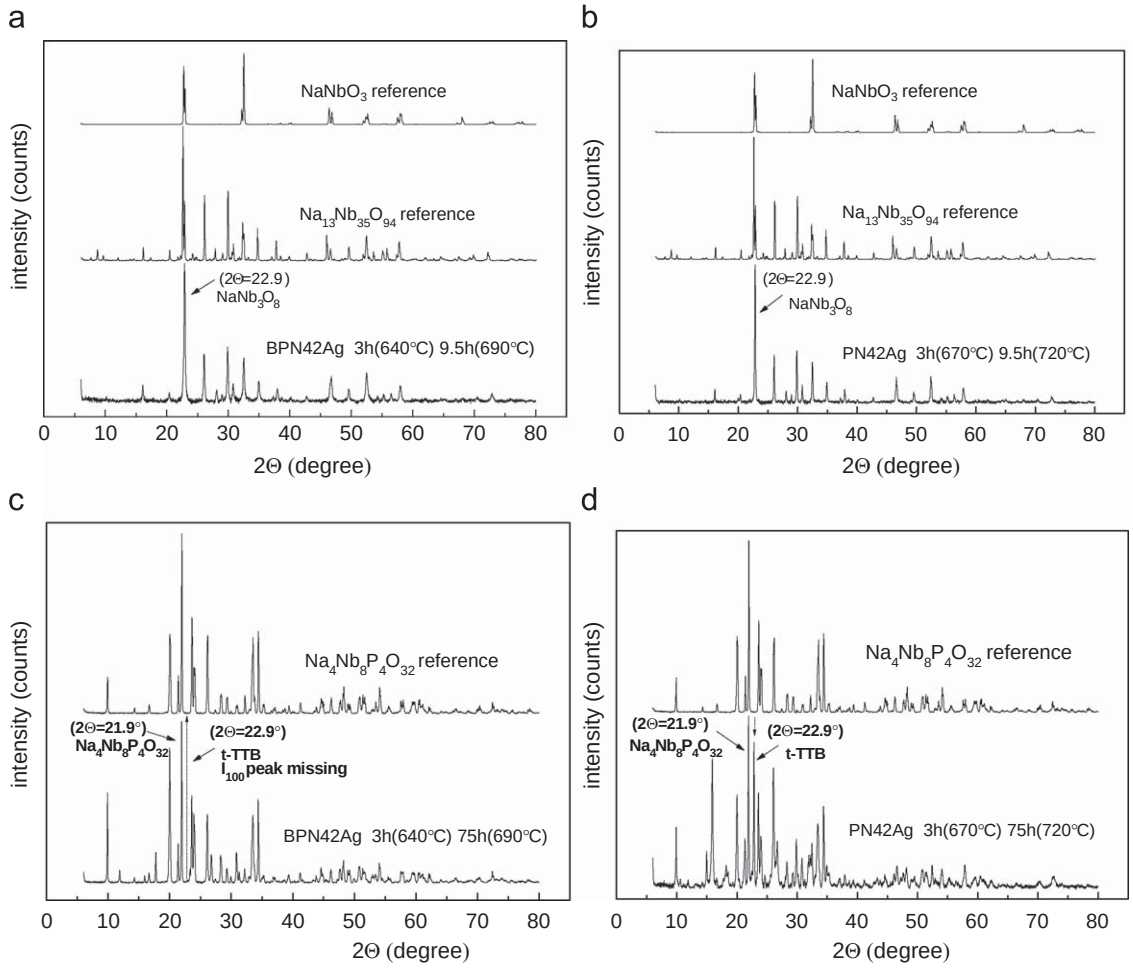

Fig. 3. XRD patterns of reference phases obtained from solid state reaction and for glasses following nucleation and crystallization heat treatments.

previously (Fig. 3c and d), *t*-TTB has totally disappeared in the borophosphate glasses. In Fig. 4a and b, one can expect that the curves overlap before observing a decreasing slope at longer crystallization duration which corresponds to the disappearing of the *t*-TTB phase and the formation of the $Na_4Nb_8P_4O_{32}$ compound.

3.3. Optical transparency

Transmission spectra have been collected on the different samples on about 1 mm thick disk. Experiments have been performed on both niobium phosphate and borophosphate glasses for silver doped and undoped glasses for different heat treatments. Similar results have been obtained for both glass systems. As shown in Fig. 5, no change can be observed for BPN42Ag and BPN42 after a nucleation treatment of 3 h. After nucleation and second heat treatment longer that 1 h, a lower transparency can be first distinguished in the blue region of the spectrum and then in all the spectral range measured. For glasses containing silver ions, the phenomenon is enhanced. After 2.5 h, significant scattering is observed.

3.4. Raman spectroscopy

Raman spectra have been collected for both matrices. Once again, both matrices exhibit same features. The results obtained for the phosphate matrix are presented in Fig. 6. No signal attributed to boron ions presence can be distinguished. Main contributions are associated to NbO_6 skeleton associated vibrations. Three bands can be noticed at 900, and 830 and at 650 cm^{-1} previously attributed, respectively, to Nb–O short bonds in distorded NbO_6 octahedra, to corner shared NbO_6 octahedra and finally, to NbO_6 associations that could be compared to tungsten bronze like structure [13,18]. Assignment of Raman bands below 300 cm^{-1} is still unclear. For all glasses, phosphate and borophosphate matrices, nucleation thermal treatments have been carried out. On the first stage of crystallization thermal treatment at 720 °C, the bands at 900 and at 830 cm^{-1} decrease in relative intensity as compared to the band centred around 650 cm^{-1}. One can also notice, as discussed by Malakho et al., on niobium borophosphate glasses a progressive shift of the band maximum to higher wavenumber [8]. A similar frequency shift was reported in infrared spectra by Dussauze et al. on niobium borophosphate glasses for Nb_2O_5 concentration above 45% [19]. Such a shift in Raman or IR could be attributed to a progressive distortion of the niobate network.

Raman spectra of the crystalline powders the $Na_{13}Nb_{35}O_{94}$ and $Na_4Nb_8P_4O_{32}$ have been also collected. Fig. 6 shows that the main features measured for $Na_{13}Nb_{35}O_{94}$ compound is observed at 650 and at 720 cm^{-1} and that no significant band can be seen above 800 cm^{-1}. For $Na_4Nb_8P_4O_{32}$, a main vibration feature is observed at 680 cm^{-1} with a shoulder at around 600 cm^{-1}. Distinct peaks are measured above 750 cm^{-1}.

For long crystallization heat treatments on glasses, as shown in Fig. 6b, the main features observed on the vitro ceramic spectrum

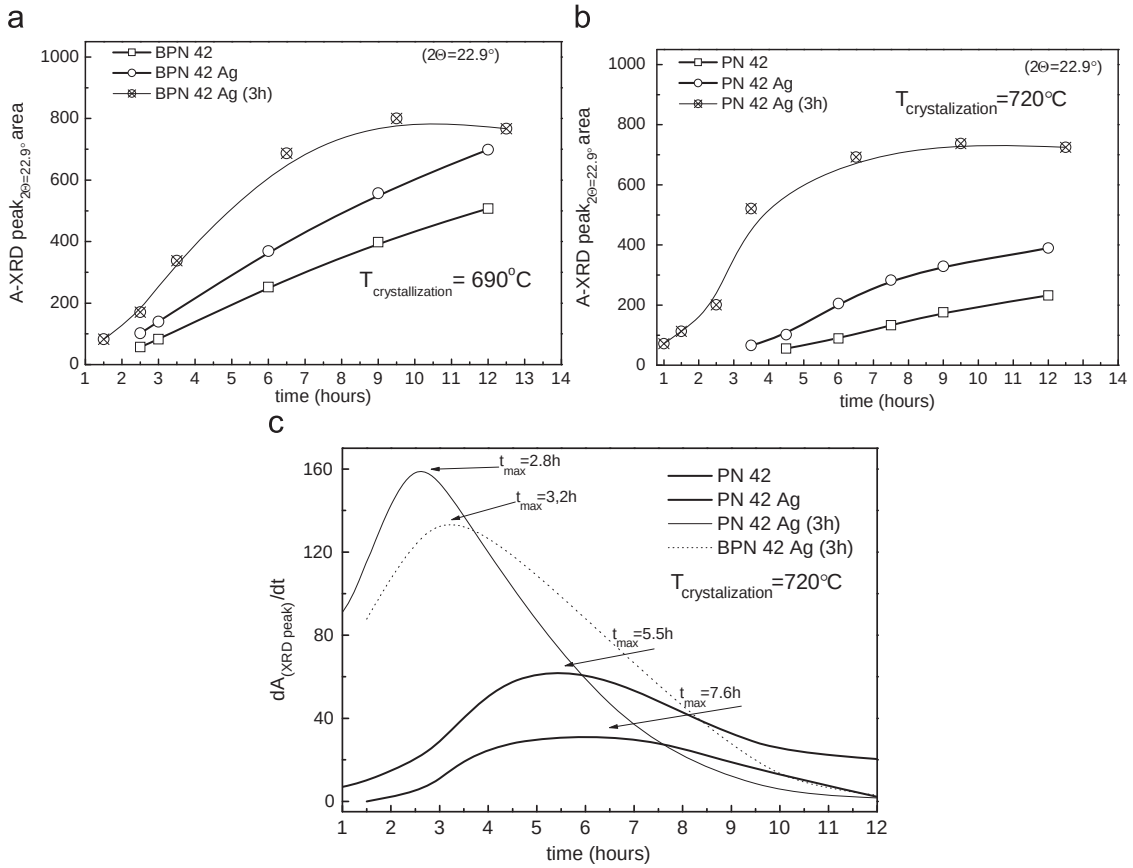

Fig. 4. Evolution of the integrated area under the diffraction peak at $2\theta = 22.9^\circ$ corresponding to the *t*-TTB phase $Na_{13}Nb_{35}O_{94}$ versus the second heat treatment duration for sodium and niobium borophosphates (a) and phosphates (b) for silver undoped and doped glasses and for silver doped glasses and 3 h nucleation heat treatment. Evolution of the derivative of the integrated area under the diffraction peak at $2\theta = 22.9^\circ$ (c).

correspond to the features observed on the spectrum collected on crystalline powder of the $Na_4Nb_8P_4O_{32}$ phase.

3.5. SEM

Scanning electron microscopy (SEM) images have been obtained on polished niobium phosphate glasses, PN42Ag and PN42Ag (3 h). For this last one, pictures are shown before and after a 1 h heat treatment at 720 °C. Prior to HRSEM investigations, all samples have been etched by HCl (1 M) in order to reveal surface morphology due to phase separation and presence of crystallites. In Fig. 7, are shown pictures obtained on PN42Ag (3 h) (a) and on a heat treated sample (b) and (c), (b) and (c) corresponding to two different magnifications. No visible feature can be seen on the surface of the initial PN42Ag (3 h) glass while a clear morphology traduced by selective etching of the acid can be distinguished after heat treatment. In the different area, exhibiting clearer contrast with size about 100 nm, bright spots with sharp edges could be assigned to crystallites.

4. Discussion

Silver addition in sodium phosphate and borophosphate containing 0.42 molar fraction of niobium oxide increases the crystallisation rate of the glass, leading in the early stage, to a *t*-TTB crystalline structure ($Na_{13}Nb_{35}O_{94}$). The mechanism at the origin of such effect is not clear. No plasmon surface resonance has been measured using optical transmission spectroscopy at any stage of the different nucleation and growth processes of the sodium niobate phase. One can suspect that the first phase formed is a silver niobate phase since silver can occupy the sodium site in the crystallite and may form $Ag_{13}Nb_{35}O_{94}$ or a solid solution $Na_{13(1-x)}Ag_{13x}Nb_{35}O_{94}$. The precipitation of these crystallites could behave as a seed for the growth of the sodium niobate phase.

As compared to silicate matrices in which sodium niobate $NaNbO_3$ phase have been obtained after crystallization, the sodium phosphate and sodium borophosphate matrices lead to opalescent materials after few hours of crystallization. According to Zhilin et al., in silicate systems, the process of crystallites formation is first described by a metastable phase separation with formation of two phases, a silicate phase and a sodium and niobium rich region, and secondly by precipitation of $NaNbO_3$ nanocrystals in the last region [4]. The same authors have also proposed that within the glass network, before any crystallization processes, "Crystal motifs" regions exist for composition with large niobium concentration. Such "Crystal motifs" are described as crystalline ordering of 2–3 coordination spheres around niobium ions with no phase boundary. In silicate and phosphate or borophosphate glasses similar Raman spectral features attributed to NbO_6 arrangements have been observed. Non linear optical (NLO) measurements on the samples exhibit in both case enhancement of the Kerr effect which has been attributed to the presence of NbO_6 TTB "structure type" in the glasses which can give rise to vibrational contribution to the fast index variation [4,7]. By considering acid etching on polished surfaces of phosphates and HRSEM investigations, one can observed that after nucleation and 1 h crystallization treatment, the surface of the glass is no more homogeneous. Different zones (dimensions

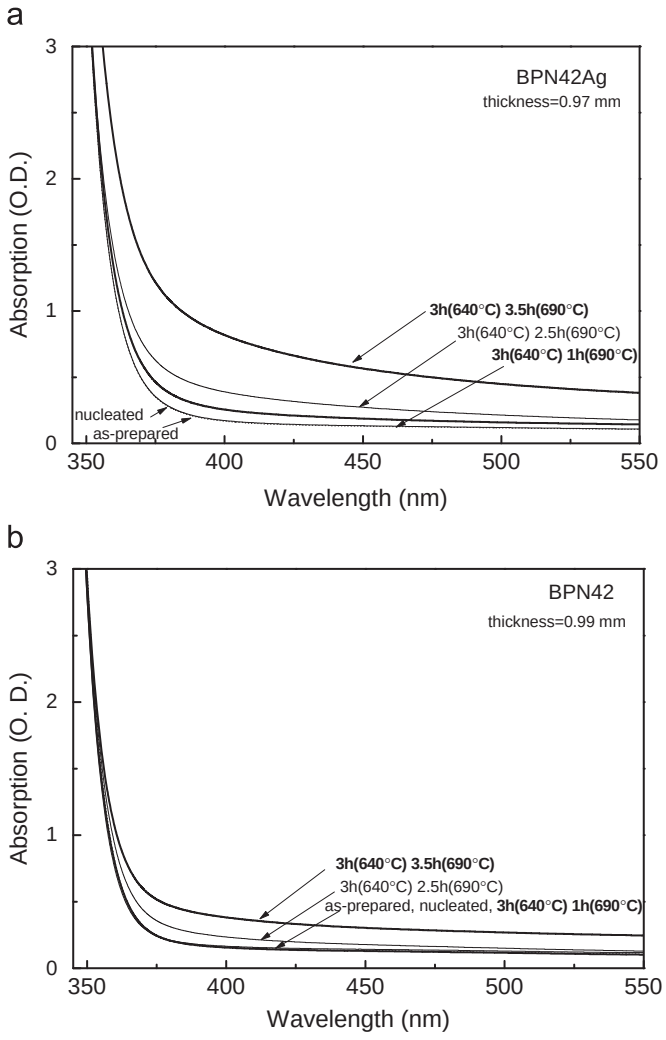

Fig. 5. Absorbance spectra of silver doped (a) and silver undoped (b) sodium and niobium borophosphate glasses for 3 h nucleation heat treatment and different durations of crystallization treatment.

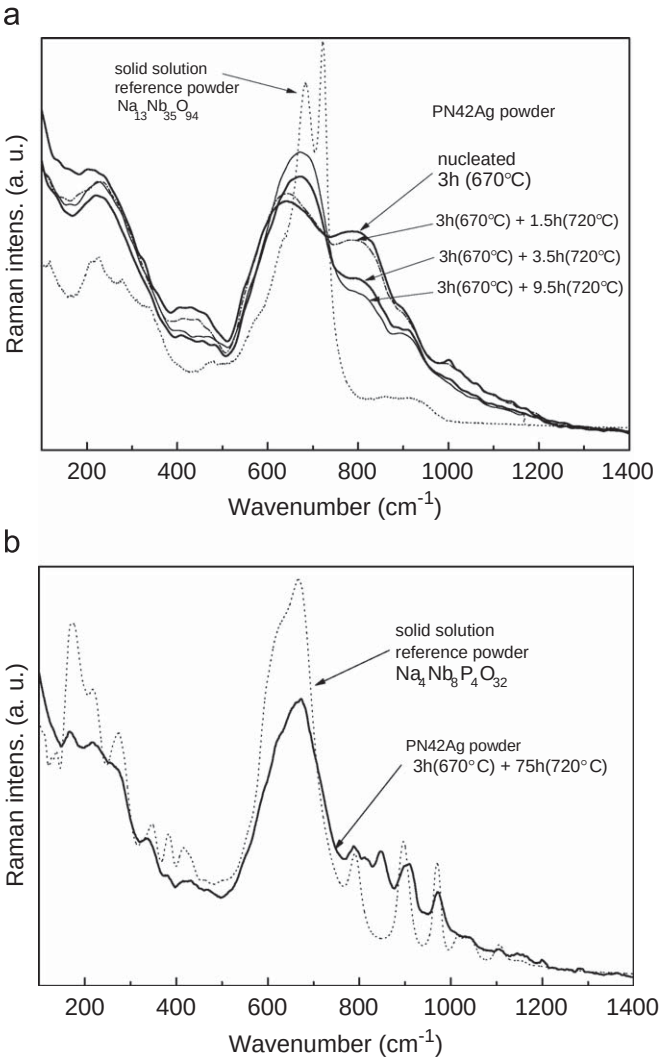

Fig. 6. Raman spectra collected on reference compound $Na_{13}Nb_{35}O_{94}$ and sodium and niobium glasses following heat nucleation heat treatment and different duration of crystallization treatments (a), and for reference compound $Na_4Nb_8P_4O_{32}$ and for sodium and niobium phosphate glass after 3 h nucleation heat treatment and long crystallization treatment.

larger than 100 nm), with inside small bright dots attributed to crystallites can be distinguished. As observed for silicates by Zhilin et al., one can suspect a vitreous phase separation prior crystallization around the "crystal motifs" formed by 3D NbO_6 corner shared octahedral [4]. In silicates, it is reported that the rich sodium and niobium region are expected to be much smaller due to the high viscosity of the SiO_2 rich region. In phosphate/borophosphate matrices, *t*-TTB ($Na_{13}Nb_{35}O_{94}$) may play the same role as $NaNbO_3$ in silicates. One can make the hypothesis that two regions are formed: a phosphate/borophosphate zone and a sodium–niobium oxide region. The formation of *t*-TTB indicates that the Nb/Na ratio in sodium–niobium rich region is higher than in the silicate glass matrices even though the Nb/Na ratio in the based glass composition are quite similar. Consequently, it can be suggested that, in comparison with sodium–niobium oxide regions, the phosphate rich-zone is stabilized by a significant amount of sodium. Sodium ions remain present in this region during the crystallization process keeping in the phosphate rich region a low viscosity. Such effect could be compatible with the formation of large niobium rich region where the precipitation of $Na_{13}Nb_{35}O_{94}$ crystalline phase in a Nb_2O_5–$NaNbO_3$ type phase diagram could take place. Accordingly to DSC thermal analysis, the formation of the two regions starts during the nucleation treatment as shown by the shortening of the difference $T_x - T_g$. Silver addition is accelerating the phenomenon. Difference of ionic mobility of silver versus sodium could be at the origin of the phase separation, and if so, could be an important parameter for controlling the phase separation. In the borophosphate/phosphate matrix, because of the lower viscosity, the *t*-TTB crystallites might react after long heat treatments and interact with the phosphate-rich part of the material to contribute to the precipitation of $Na_4Nb_8P_4O_{32}$.

The opalescent character of the material after crystallization thermal treatment seems to be driven first by the vitreous phase separation with region larger than 100 nm. The scattering, in that case would come from linear refractive index variation between rich phosphate/borophosphate and niobium zones. Crystallites of the *t*-TTB phase with lower size than 100 nm are most likely occurring after the phase separation in the rich niobium oxide zones.

5. Conclusion

Addition of silver in sodium–niobium phosphate or borophosphate glasses is affecting the rate of crystallization of the

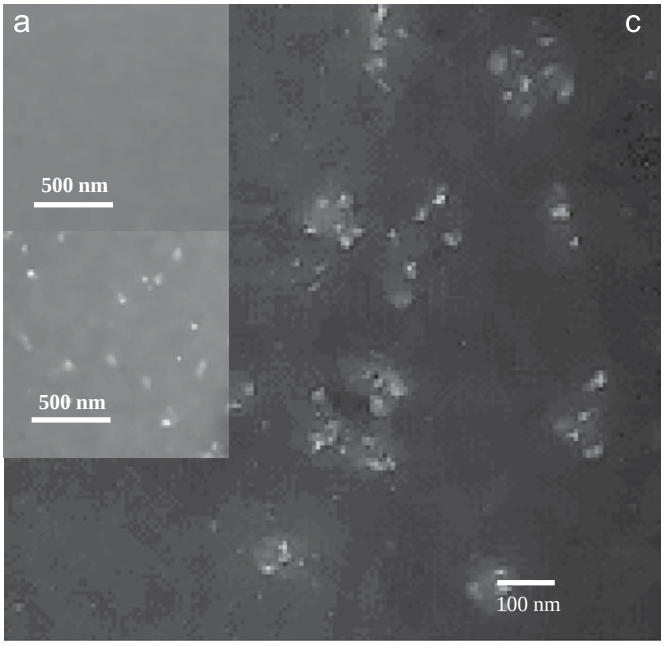

Fig. 7. HRSEM micrograph of acid etched surface of silver doped sodium and niobium phosphate glass after 3 h nucleation heat treatment before (a) and after (b), (c) 1 h crystallization treatment at 720 °C.

materials while keeping same crystalline phase precipitation in doped and undoped glasses. For 0.5 molar percent of silver added, no effect on the glass transition temperature could be evidenced but significant shortening of the difference $T_x - T_g$ was demonstrated. Silver addition in the glasses favours the phase separation leading to sodium phosphate and sodium niobate rich regions. Formation of $Na_{13}Nb_{35}O_{94}$ crystalline phase as opposed to $NaNbO_3$ has been attributed to important sodium concentration remaining in the phosphate/borophosphate rich region leading to crystallite formation in a Nb_2O_5–$NaNbO_3$ system.

Acknowledgments

This work has been supported by the Agence Nationale de la Recherche (grant ANR-05-BLAN-0212-01), the CNRS (PICS grant 3179), the Aquitaine Region, the GIS AMA, the NSF and a FACE grant from the French Embassy in the US.

References

[1] H. Jain, Ferroelectrics 306 (2004) 111–127;
T. Berthier, V. Fokin, E. Zanotto, J. Non-Crystalline Solids 354 (2008) 1721–1730.
[2] E.M. Vogel, J. Am. Ceram. Soc. 72 (1989) 719–724.
[3] H. Jain, Ferroelectrics 306 (2004) 111–127.
[4] A.A. Zhilin, G.T. Petrovskii, V.V. Golubkov, A.A. Lipovskii, D.K. Tagantsev, B.V. Tayarintsev, A.A. Shepilov, J. Non-Crystalline Solids 345&346 (2004) 182–186.
[5] N.V. Golubev, V.N. Sigaev, S.Yu. Stefanovich, T. Honma, T. Komatsu, J. Non-Crystalline Solids 354 (2008) 1909–1914.
[6] M. Dussauze, E. Fargin, M. Lahaye, V. Rodriguez, F. Adamietz, Opt. Express 13 (11) (2005) 4064–4069.
[7] A. Royon, L. Canioni, B. Bousquet, M. Couzi, V. Rodriguez, C. Rivero, T. Cardinal, E. Fargin, M. Richardson, K. Richardson, Phys. Rev. B 75 (1) (2007) 04207.
[8] A. Malakho, M. Dussauze, E. Fargin, B. Lazoryak, V. Rodriguez, F. Adamietz, J. Solid State Chem. 178 (2005) 1888–1897.
[9] A. Karamanov, P. Pisciella, M. Pelino, J. Eur. Ceram. Soc. 19 (1999) 2641–2645.
[10] G. Dantelle, M. Mortier, D. Vivien, G. Patriarche, J. Mater. Res. 20 (2) (2005) 472–481.
[11] S. Stookey, Ind. Eng. Chem. 41 (1949) 856–861.
[12] L.B. Glebov, Opt. Mater. 25 (2004) 413–418.
[13] T. Cardinal, E. Fargin, G. Le Flem, M. Couzi, L. Canioni, P. Segonds, L. Sarger, A. Ducasse, F. Adamietz, Eur. J. Solid State Inorg. Chem. 33 (1996) 597–605.
[14] A.W. Hewat, Ferroelectrics 7 (1974) 83–85.
[15] G. Costentin, M.M. Borel, A. Grandin, A. Leclaire, B. Raveau, Mater. Res. Bull. 26 (1991) 1051–1057.
[16] D.C. Craig, N.C. Stephenson, J. Solid State Chem. 3 (1971) 89–100.
[17] J. Rodriguez-Carvajal, Fullprof: a program for Rietveld refinement and pattern matching analysis, in collected abstract of powder diffraction meeting, Toulouse, France, 127 (1990);
J. Rodriguez-Carvajal, Physica B 192 (1993) 55–69.
[18] A.A. Lipovskii, D.K. Tagantsev, A.A. Vetrov, O.V. Yanush, Opt. Mater. 21 (2003) 749–757.
[19] M. Dussauze, E.I. Kamitsos, E. Fargin, V. Rodriguez, J. Phys. Chem. C 111 (2007) 14560–14566.